Influence of stellar properties on disc photoevaporation

Giovanni Picogna[1] ⓘ, Ercolano Barbara[1,2] ⓘ, and Catherine Espaillat[3] ⓘ

[1] Universitäts-Sternwarte, Ludwig-Maximilians-Universität München, Scheinerstr. 1, D-81679 München, Germany
    e-mail: picogna@usm.lmu.de, ercolano@usm.lmu.de
[2] Excellence Cluster Origins, Boltzmannstrasse 2, D-85748 Garching bei München, Germany
[3] Department of Astronomy & Institute for Astrophysical Research, Boston University, 725 Commonwealth Avenue, Boston, MA 02215, USA
    e-mail: cce@bu.edu

ABSTRACT

Key words. accretion, accretion discs – protoplanetary discs – circumstellar matter – stars: pre-main-sequence – X-rays: stars.

1. Introduction

2. Methods

We follow the approach outlined in Picogna et al. (2019) and model the photoevaporative wind by means of a set of hydrodynamical simulations.

We modelled 4 different stellar masses, ranging from $0.1 M_\odot$ to $1.0 M_\odot$ which, together with the $0.7 M_\odot$ studied in Picogna et al. (2019), allow us to study in detail the stellar mass dependance on the mass-loss rates due to photoevaporative winds. The initial parameter adopted in the different runs are summarized in Table 1 and the disc is initially extending out to 400 au.

2.1. Thermal calculations

The gas temperatures are calculated using the gas photoionization and dust radiative transfer code MOCASSIN (Ercolano et al. 2003, 2005, 2008b), that solves the heating and cooling terms for various physical and irradiation properties at the thermal equilibrium. We irradiate a slab of gas with solar abundances (Asplund et al. 2005) depleted by the amount locked in dust grains (Savage & Sembach 1996), using a X-ray+EUV (XEUV) spectrum (see Ercolano et al. (2008a, 2009) for details). The spectrum was generated by the plasma code PINTofALE (Kashyap & Drake 2000), assuming an emission distribution derived for CVn binaries (Sanz-Forcada et al. 2002) which fits Chandra spectra of T Tauri stars (Maggio et al. 2007). Spectra with different hardness do not have a measurable effect on the cumulative mass-loss rate, but they can change the global disc evolution by launching a thermal wind deeper within the disc, thus opening a gap at larger radii (see Picogna, Monsch, Ercolano, Drake, in prep.). A depletion in Carbon with respect to solar abundance can, on the other hand, have a considerable effect increasing the cumulative mass-loss rates of the photoevaporative wind (Wölfer et al. 2019).

Based on the results of Owen et al. (2010); Picogna et al. (2019) we parameterise the gas temperature based on gas local properties (number density, n) via the ionization parameter
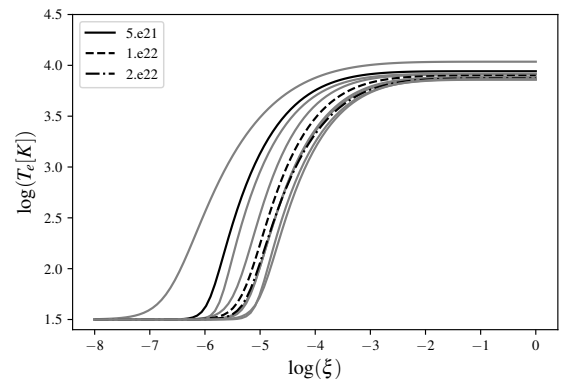
$$\xi = \frac{L_X}{nR^2}, \tag{1}$$

Fig. 1. Temperature as a function of the ionization parameter, where 3 selected column densities are highlighted.

where L_X is the X-ray luminosity of the central star in erg/s, and R is the cylindrical radius; and column density (N), $T(\xi, N)$. We then utilise them to calculate the gas temperature up to the maximum penetration depth of the X-ray irradiation, $N = N_X = 2.5 \cdot 10^{22}$ pp/cm^2, during the hydrodynamical simulations. We divide the parameterisation in 20 slabs equally spaced betweem $N = 2.5 \cdot 10^{21}$ pp/cm^2 and N_X. In Figure 1, taken from Picogna et al. (2019), we illustrate the behavior of the temperature dependance on the ionization parameter. For a detailed analytical description of the different functions the reader is referred to Picogna et al. (2019).

The dust temperatures and initial density structure are calculated using the D'Alessio Irradiated Accretion Disk (DIAD) radiative transfer models (D'Alessio et al. 1998, 1999, 2001, 2005, 2006), that best fit the median spectral energy distribution (SED) in Taurus. The gas temperatures is assumed to be completely coupled to the dust temperature for $N > N_X$.

Table 1. Star and disc properties

$M_\star$ [$M_\odot$]	$R_\star$ [$R_\odot$]	ST	$L_\star$ [$L_\odot$]	L_X [10^{29} erg/s]	$T_\star$ [K]	M_d [$M_\odot$] (%)	R_{in} [au]	R [cells]
1.0	2.615	K6	2.335	20.4	4278	0.0444 (4.4)	0.445	412
0.5	2.125	M1	0.9288	7.02	3771	0.0363 (7.3)	0.2225	449
0.3	2.310	M5	0.6887	3.20	3360	0.0292 (9.7)	0.1335	477
0.1	1.055	M6	0.08559	0.589	2928	0.0264 (26.4)	0.0445	535

2.2. Hydrodynamical model

We performed a set of hydrodynamical simulations using the PLUTO code (Mignone et al. 2007), adopting a spherical coordinate system centred on to the star. The grid is logarithmically spaced in the radial direction, in order to have better resolution in the inner region of the disc, where photo-evaporation is mostly effective. At the same time, it allows us to model the disc out to large radii (R_{out} = 1000 au) without increasing strongly our computational costs and preventing boundary effects that can affect the stability of the wind flow. For a detailed discussion of the numerical artifacts induced by the grid outer boundary, the reader is referred to Picogna et al. (2019). The grid is spaced linearly in the polar direction to maximize the resolution at the wind launching region.

We initially evolve the system for 100 orbits at 10au without stellar irradiation, in order to reach a quasi-hydrostatic equilibrium. Then, we switch on the stellar heating (applied through a parameterisation from the radiative transfer simulation, as explained above) and continue to evolve the system until the cumulative mass-loss rate and gas streamline in the wind have reached a stable configuration.

3. Results

3.1. Primordial discs

3.1.1. Sonic surface

The analysis of **?** is based on the assumption that the properties of the mass-flux can be determined at the sonic surface, and that the sound speed is roughly given by the Parker value

$$c_s^2 = \frac{GM_\star}{2R} \tag{2}$$

An important assumption is that the height of the sonic surface is not much larger than its cylindrical radius ($z_s \not\gg R$)

4. Conclusions

1. PE exists.

References

Asplund, M., Grevesse, N., & Sauval, A. J. 2005, Astronomical Society of the Pacific Conference Series, Vol. 336, The Solar Chemical Composition, ed. I. Barnes, Thomas G. & F. N. Bash, 25

D'Alessio, P., Calvet, N., & Hartmann, L. 2001, ApJ, 553, 321

D'Alessio, P., Calvet, N., Hartmann, L., Franco-Hernández, R., & Servín, H. 2006, ApJ, 638, 314

D'Alessio, P., Calvet, N., Hartmann, L., Lizano, S., & Cantó, J. 1999, ApJ, 527, 893

D'Alessio, P., Cantö, J., Calvet, N., & Lizano, S. 1998, ApJ, 500, 411

D'Alessio, P., Hartmann, L., Calvet, N., et al. 2005, ApJ, 621, 461

Ercolano, B., Barlow, M. J., & Storey, P. J. 2005, MNRAS, 362, 1038

Ercolano, B., Barlow, M. J., Storey, P. J., & Liu, X. W. 2003, MNRAS, 340, 1136

Ercolano, B., Clarke, C. J., & Drake, J. J. 2009, ApJ, 699, 1639

Ercolano, B., Drake, J. J., Raymond, J. C., & Clarke, C. C. 2008a, ApJ, 688, 398

Ercolano, B., Young, P. R., Drake, J. J., & Raymond, J. C. 2008b, ApJS, 175, 534

Kashyap, V. & Drake, J. J. 2000, Bulletin of the Astronomical Society of India, 28, 475

Maggio, A., Flaccomio, E., Favata, F., et al. 2007, ApJ, 660, 1462

Mignone, A., Bodo, G., Massaglia, S., et al. 2007, ApJS, 170, 228

Owen, J. E., Ercolano, B., Clarke, C. J., & Alexand er, R. D. 2010, MNRAS, 401, 1415

Picogna, G., Ercolano, B., Owen, J. E., & Weber, M. L. 2019, MNRAS, 487, 691

Sanz-Forcada, J., Brickhouse, N. S., & Dupree, A. K. 2002, Astronomical Society of the Pacific Conference Series, Vol. 277, Quiescent and Flaring Coronal Structure in RS CVn Stars, ed. F. Favata & J. J. Drake, 585

Savage, B. D. & Sembach, K. R. 1996, ApJ, 470, 893

Wölfer, L., Picogna, G., Ercolano, B., & van Dishoeck, E. F. 2019, MNRAS, 490, 5596